Plasmonic band gaps of structured metallic thin films evaluated for a surface plasmon laser using the coupled-wave approach

Takayuki Okamoto,[1,*] Janne Simonen,[1,2] and Satoshi Kawata[1,3]
[1]*RIKEN (The Institute of Physical and Chemical Research), Hirosawa, Wako, Saitama 351-0198, Japan*
[2]*Optoelectronics Research Centre, Tampere University of Technology, P.O. Box 692, FI-33101 Tampere, Finland*
[3]*Department of Applied Physics, Osaka University, Yamada-oka, Suita, Osaka 565-0871, Japan*
(Received 18 October 2007; revised manuscript received 20 January 2008; published 17 March 2008)

The behavior of plasmonic band gaps appearing in the dispersion relations of surface plasmons for periodically corrugated thin silver films is theoretically investigated by using the rigorous coupled-wave approach. The structures have one-dimensional rectangular corrugations with 25%, 50%, and 75% fill factors and support both long-range and short-range surface plasmon band gaps. A unified explanation for the necessary conditions for opening these band gaps, as well as intermode band gaps, is given. The radiation characteristics of the surface plasmons at the edges of these band gaps are also analyzed. Based on the findings, the optimal structure for a plasmonic band gap laser is presented.

DOI: 10.1103/PhysRevB.77.115425 PACS number(s): 73.20.Mf, 78.20.Bh, 78.67.−n

I. INTRODUCTION

In the last decade, plasmonics has emerged as a key word in nanophotonics. Surface plasmons are electromagnetic surface waves confined onto a metal-dielectric interface and provide both high localization and enhanced field intensities in the nanoscale. These properties are attractive for applications in areas such as nano-optical circuits, nanoimaging, nanoanalysis, and nanobiosensors.[1–3] However, surface plasmons suffer from absorption loss while propagating at a metal-dielectric interface. To overcome the absorption loss, active materials are combined.[4–6] In some cases, this has even enabled the amplification of surface plasmons.[7,8]

Amplifying surface plasmons has opened up a new way for constructing a lasing device. We have previously proposed a plasmonic band gap laser that comprises a two-dimensional periodically corrugated metal surface coated with a gain medium.[9] The corrugation opens band gaps in the dispersion relation and provides coupling of the plasmon mode with free-space radiation. The wide band gap lowers the group velocity of the surface plasmons, resulting in a decrease of the lasing threshold.[10] We have employed long-range surface plasmon (LRSP) modes, which are plasmon modes supported in optically thin metallic films. Using LRSP modes dramatically reduces the absorption loss. However, another source of losses that remains is the scattering or radiation of photons at the periodic corrugation.

There will not be any radiation or coupling to photons from surface plasmons if the surface of the metal film is perfectly flat because the wave vector of the surface plasmon is always larger than that of the free-space radiation in the adjacent dielectric medium. In other words, the dispersion curve of the surface plasmon always lies outside the light cone. Radiation may occur if the metal surface is corrugated, resulting in losses. Similar to the Fabry–Pérot laser cavity, in which the transmittance of the cavity mirror is nearly zero, coupling efficiency from plasmons to free-space radiations should be small enough for a plasmonic band gap laser.[11]

In this paper, we investigate the dispersion relations and radiation characteristics of thin silver films with several types of corrugations using numerical simulations. The characteristics of band gaps in corrugated metal thin films have been previously studied by Hooper and Sambles.[12] We deal with the plasmonic phenomena arising in such structures as metallic thin films with symmetrically and antisymmetrically corrugated interfaces with various phase differences on both sides and metallic thin films with one flat and one corrugated interface on each side. Similar structures have been investigated by Gérard *et al.*[13] in the case of resonant transmission. We show the structures needed to open up surface plasmon band gaps with minimized radiation losses. These structures are the key requirements for achieving a plasmonic band gap laser.

II. MODEL AND ANALYSIS METHOD

The studied grating profile is rectangular; in other words, the gratings are binary. For the simulations, we used the rigorous coupled-wave approach (also known as the Fourier modal method), which is well suited for analyzing binary metallic gratings, provided that care is taken in the implementation to avoid convergence problems.[14–16] For simplicity, we will investigate periodically corrugated metal films with one-dimensional geometries.

Silver was our material of choice as it had the smallest absorption losses in the visible region, and the dielectric function was obtained from Johnson and Christy.[17] We fixed the grating period, the maximum thickness, and the groove depth throughout this paper to 600, 50, and 10 nm, respectively. The thickness of 50 nm is small enough to provide coupling of the modes on each interface, giving rise to long- and short-range plasmon modes. The dielectric constant of the ambient was assumed to be unity.

The number of diffraction orders taken into account in our calculations was 41 (orders between +20 and −20). This was found to be enough to provide both reasonable accuracy and short calculation times—even if we would include more than 41 diffraction orders, qualitative behavior of the dispersion relation would not change.

We investigated gratings with three different fill factors (duty ratios), i.e., 25%, 50%, and 75%. It has been shown that the second harmonic Fourier component ($2K$, where K is the grating vector) of the grating profile plays a crucial role in opening plasmonic band gaps.[18] The amplitude of the $2K$ component depends on the fill factor. Both 25% and 75% fill factors produce a second harmonic component with maximum amplitude, while gratings with a 50% fill factor have no $2K$ components. With respect to the fill factors of both the top and bottom film interfaces, we categorized the examined grating structures into three groups.

In group I, the fill factor of the bottom interface is identical to that of the top interface, and the phase between the corrugations on both interfaces is varied. We analyzed three different phases: i.e., 0, $\pi/2$, and π. All the possible combinations of the fill factor and the phase difference result in nine distinct structures.

In group II, the fill factor of the bottom interface is complementary to that of the top interface, e.g., when the fill factor of the top interface is 25%, that of the bottom interface is 75%. The phase difference between top grating and bottom grating is also 0, $\pi/2$, or π, resulting in nine structures in total.

In group III, one of the interfaces is flat, giving us three structures with different fill factors. Since in addition to the appearance of band gaps, we are also interested in coupling efficiency between incident light and plasmons, we simulated illuminating the structures from both the flat and the corrugated sides.

III. RESULTS

We obtained the dispersion relations of the surface plasmon modes by calculating the absorptance as a function of energy E of a p-polarized incident plane wave and its in-plane wave vector k_x. The dispersion relation is represented by the loci of the maxima of absorptance. Figure 1 shows the results for group I, i.e., the structures in which the top and bottom interfaces have the same fill factors. Figure 2 presents the results for group II, i.e., the structures with complementary fill factors on each interface. Figure 3 shows the results for group III, i.e., the structures in which one interface is flat. The absorptance is normalized in each figure.

As mentioned above, the silver films we analyzed were thin enough for the surface plasmons on both interfaces to interact, resulting in two modes, i.e., the LRSP and the short-range surface plasmon (SRSP). Thus, since the plasmons on each interface are not separately excited, the observed dispersion relation does not depend on the illuminated interface. On the other hand, the coupling efficiency between the plasmons and free-space radiation does indeed depend on the structure of each interface.

To open a plasmonic band gap, there must be standing waves of surface plasmons. This requires interaction between forward and backward propagating plasmons, which is produced by gratings that have a $2K$ component.[18] As expected, since gratings with a 50% fill factor have no $2K$ components, no plasmonic band gaps are seen for these structures regardless of the relative phase of the gratings on each interface.

However, a careful observation of the dispersion figures reveals something more—there are, in fact, very small gaps produced by structures B (Ref. 19) and H, but there is no gap for structure E. Since the structures have no $2K$ components, these band gaps are caused by a diffraction from the higher order Fourier components of the grating profile. In this case, the surface plasmon with k_{sp} may interact with the surface plasmon with $-k_{sp}$ through two diffraction processes, such as $k_{sp}+K-3K=-k_{sp}$. As these processes are quite weak, the band gaps are small. The reason why there is no gap in the case of structure E will be discussed later.

A. Behavior of band gaps and radiation characteristics at band edges

There are three crossing points of plasmon modes in each dispersion map. The crossing point with a higher energy at normal incidence ($k_x=0$) corresponds to counterpropagating LRSP modes, while that with a lower energy corresponds to counterpropagating SRSP modes. We call the band gaps caused by these interactions *intramode* plasmonic band gaps. The third crossing point at $k_x \neq 0$ corresponds to a LRSP mode and a SRSP mode, which we call an *intermode* band gap. Whether there is a band gap at each crossing point depends on the film structure. This dependence can be explained, as described below.

First, instead of coupled modes of a thin metal film, let us consider the simpler case of a corrugated surface of a semi-infinite thick metal, which also can produce a plasmonic band gap at $k_x=0$. The energy of the standing wave on the band edge depends on the phase difference between the plasmon wave and the $2K$ Fourier component of the grating.[18] When the node of the charge distribution associated with the standing waves corresponds to the peak of the $2K$ component, the energy of the standing wave is high: ω_+. On the other hand, when the node of the charge distribution corresponds to the valley of the $2K$ component, the energy is low: ω_-. If the surface has no corrugation, the energy is in between them: ω_0. We categorize the combination of the charge distribution and the grating structure into five types, a, b, c, d, and e, as shown in Fig. 4 (note that the $2K$ component is not explicitly shown).

The radiation characteristics of the thick metal film can be explained by the parity of the incident field and the charge distribution. Since the electric field of the incident beam at normal incidence ($k_x=0$) is parallel to the grating, its parity is odd with respect to the surface profile. This incident field can only excite those standing waves of surface plasmons that have the same odd parity of the charge distribution with respect to the grating profile. Thus, in Fig. 4, only modes of types b and d can be excited at normal incidence.

Due to the reciprocity theorem, plasmons that can be optically excited also necessarily radiate. We denote this radiation characteristic as $r_{\pm}$, as shown in Fig. 4, where r_+ and r_- indicate radiative and nonradiative plasmons, respectively. By combining the energy and radiation characteristics, here we introduce a notation for each surface structure as shown in Fig. 4, i.e., $a:\omega_- r_-$, $b:\omega_+ r_+$, $c:\omega_+ r_-$, $d:\omega_- r_+$, and $e:\omega_0 r_-$.

B. Intramode plasmonic band gaps

Based on the preparations above concerning thick metal structures, let us return to plasmonic band gaps in corrugated

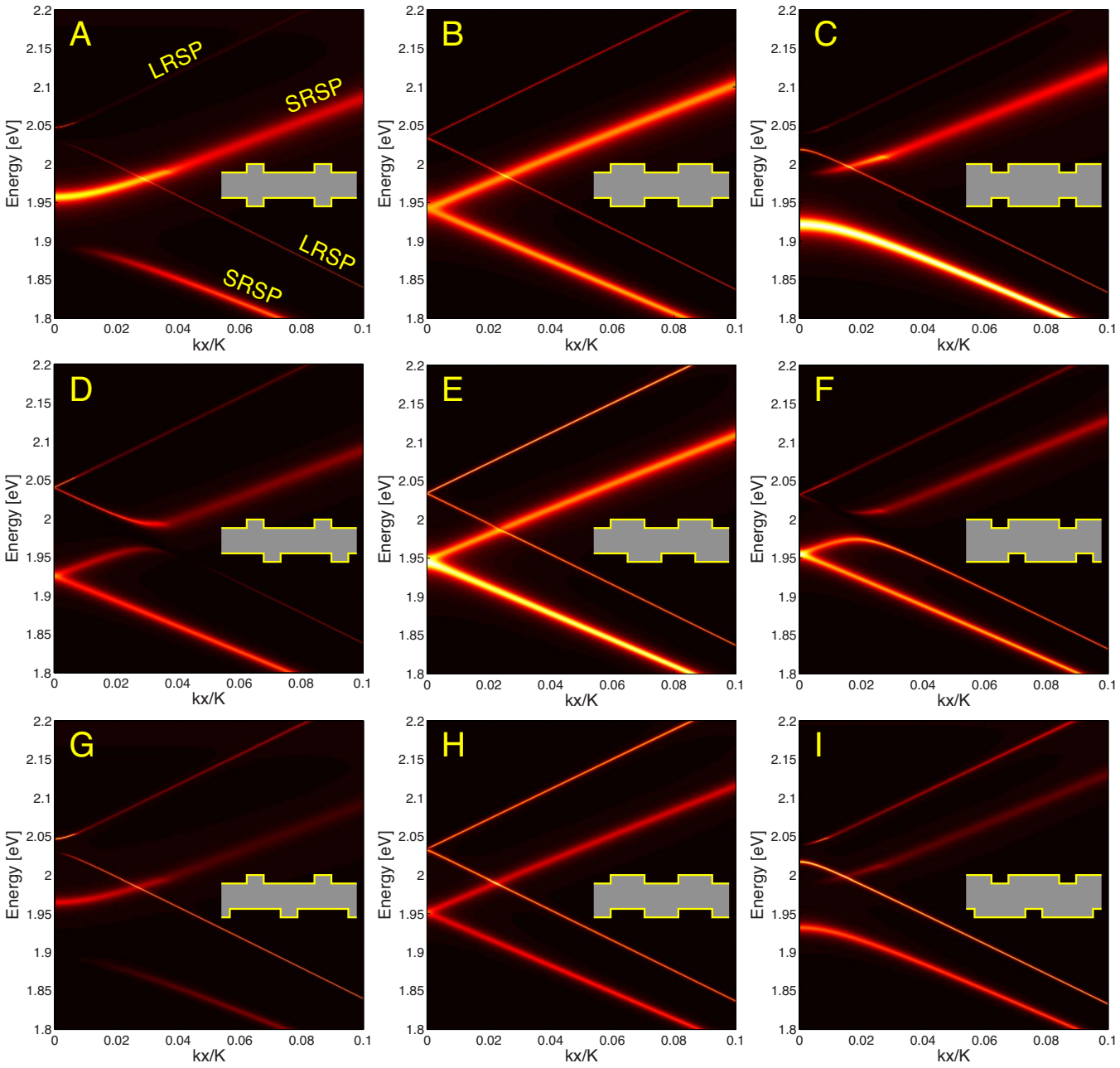

FIG. 1. (Color online) The calculated dispersion relations for the structures of group I; normalized absorptance as a function of the energy E and the in-plane wave vector k_x of incident light. The insets indicate the film structures. In this group, the fill factors of the corrugation in both interfaces are identical. The incidence is from above. Two intramode band gaps open for structures A, C, G, and I, while an intermode band gap opens for structures D and F. There are very narrow gaps at $k_x=0$ in structures B and H, but no gap in structure E.

thin films. The key to understanding the formation of the band gaps lies in the relative phase of the charge distributions between the two interfaces of the film. From this, we can deduce the possible energies of all the modes—if there is an energy difference, there will be a band gap.

In the SRSP modes, the phase difference of the charge distribution between the two interfaces $\Delta\phi$ is zero, while in the LRSP mode, the charge distribution in one interface is antiphase to that in the other interface, i.e., $\Delta\phi=\pi$. As shown in Fig. 1, in structure C, for example, the possible charge distributions at $k_x=0$ on each interface are types c and c or types d and d for both SRSP and LRSP modes, as shown in Fig. 5.

Here, we introduce another notation by representing these combinations as $[c:\omega_+r_-|c:\omega_+r_-]\rightarrow r_-\omega_{2+}r_-$ and $[d:\omega_-r_+|d:\omega_-r_+]\rightarrow r_+\omega_{2-}r_+$. In the notation $[c:\omega_+r_-|c:\omega_+r_-]\rightarrow r_-\omega_{2+}r_-$, the first c denotes the type of the mode on the top interface with energy ω_+ and the second c denotes the type of the mode on the bottom interface with energy ω_+, resulting in energy ω_{2+}.

The rule for obtaining the mode energy in the thin film case is as follows. When the energies of both interfaces are

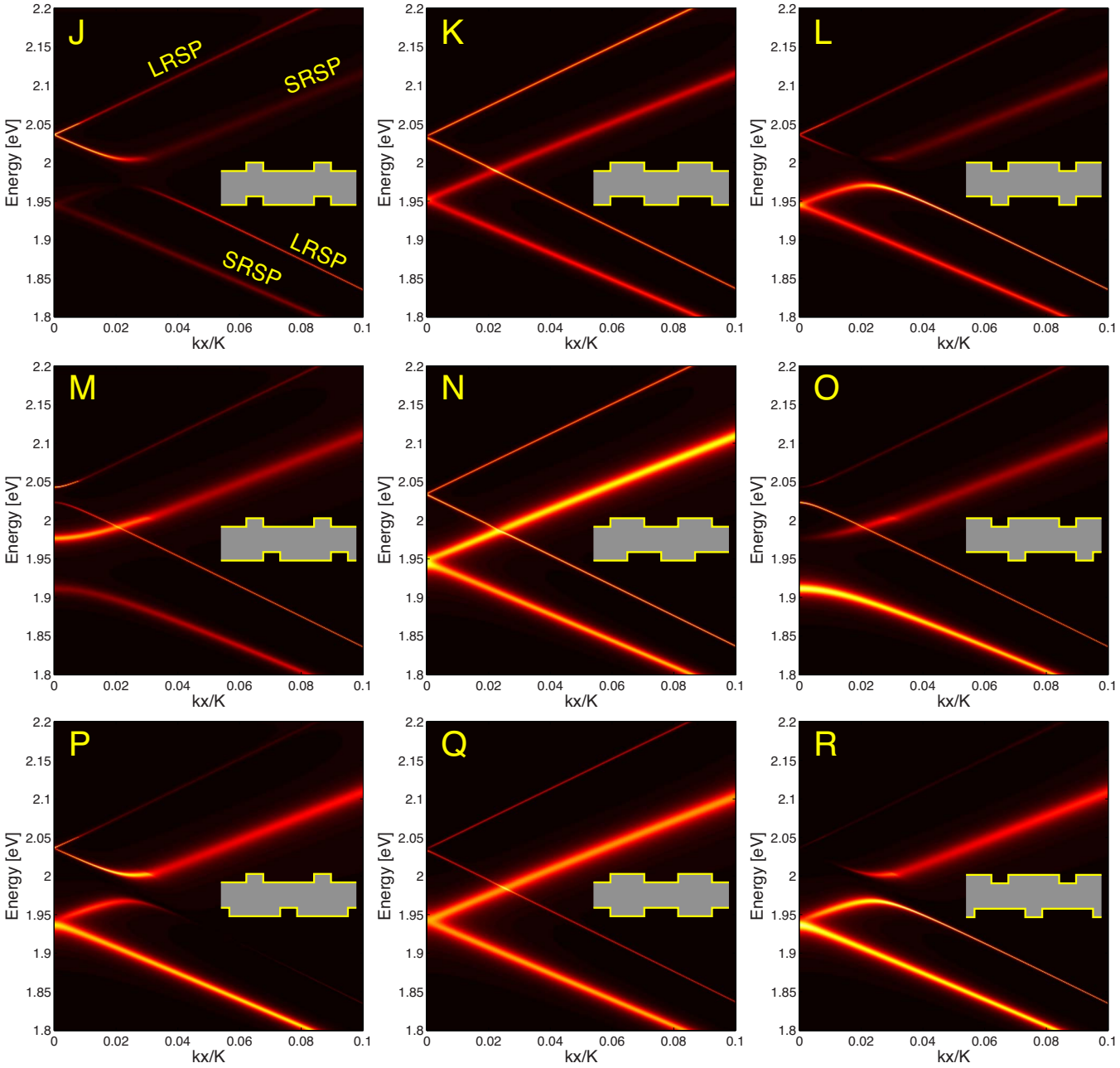

FIG. 2. (Color online) Same as Fig. 1 but now for the structures of group II. In this group, the fill factors of the corrugations of each interface are complementary. Two intramode band gaps open in structures M and O, while an intermode band gap opens in structures J, L, P, and R. There are very narrow gaps at $k_x=0$ in structures K and Q, but no gap in structure N.

ω_+ and ω_+ or ω_- and ω_-, the resultant energy becomes ω_{2+} or ω_{2-}, respectively. The energy ω_{2+} is higher than ω_+, while the energy ω_{2-} is lower than ω_-. When the energy of an interface is ω_+ or ω_- and the energy of the other interface is ω_0, the resultant energy becomes ω_+ or ω_-, respectively. The remaining combination is ω_+ and ω_-. In this case, the resultant energy is ω_0.

In structure C, since there are two possible total energies, i.e., ω_{2+} and ω_{2-}, at $k_x=0$ for both SRSP and LRSP modes, an energy gap opens for both modes. Next, let us consider structure *J*. There are also two possible combinations at $k_x=0$; $[a:\omega_- r_-|c:\omega_+ r_-] \rightarrow r_-\omega_0 r_-$ and $[b:\omega_+ r_+|d:\omega_- r_+] \rightarrow r_+\omega_0 r_+$, as shown in Fig. 6. Since both combinations have the same energy ω_0, there are no gaps.

For the case when the phase of the corrugation of one interface is shifted from that of the other interface by $\pi/2$, the possible charge distributions for both SRSP and LRSP modes are shown in Fig. 7. Since the period of the $2K$ component of the grating is π, the modes on each interface will have opposite energies; thus, the resultant energy of the mode is always ω_0. In all the $\pi/2$-phase shift films, therefore, no band gaps can open at $k_x=0$. This is also true for other fill factors, for example, for structure E.

C. Intermode plasmonic band gaps

In order to investigate the intermode plasmonic band gap at the crossing point ($k_x \neq 0$) of a LRSP mode and a SRSP

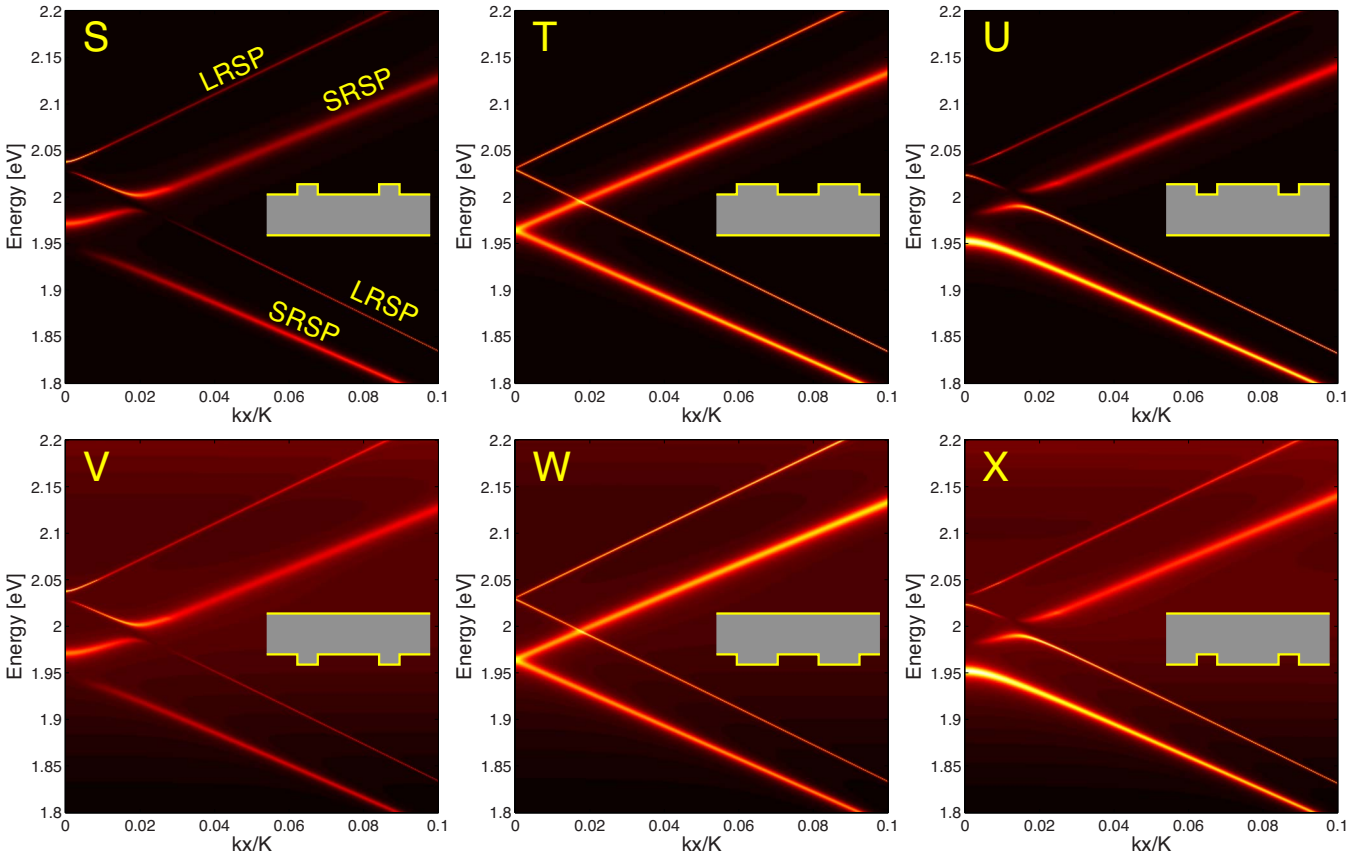

FIG. 3. (Color online) Same as Fig. 1 but for the structures of group III. In this group, one of two interfaces is flat. Two intramode band gaps and one intermode band gap open in structures S, U, V, and X, while very narrow intramode plasmonic band gaps open in structures T and W. The maximum absorptance values for the incidence from the flat interface (V, W, and X) are an order of magnitude smaller than those from the corrugated interface (S, T, and U).

mode, we calculated the electromagnetic field distribution in structure L, as shown in Fig. 2. Figures 8(a) and 8(b) show the amplitude and the phase of the excited magnetic field, respectively, at the lower edge ($k_x/K=0.0228$ and $E=1.9705$ eV) of the intermode band gap. In this calculation, 201 diffraction orders were taken into account to guarantee convergence for oblique incidence. It is recognized that the spatial phase of the standing plasmon wave on the top interface shifts from that of the bottom interface by $\pi/2$. In addition, the temporal phase of the oscillation of the standing plasmons on both interfaces also has a $\pi/2$ difference.

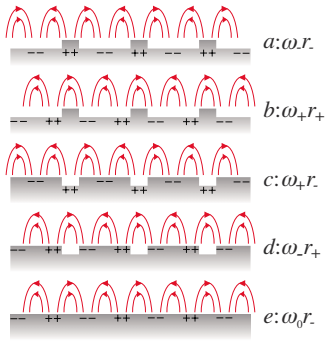

FIG. 4. (Color online) Charge distribution for standing surface plasmons in corrugated and uncorrugated metal surfaces of semi-infinite thick metals. The symbols ω_+, ω_0, and ω_- indicate relative energy of each mode: i.e., ω_+ is high, ω_0 is middle, and then ω_- is low. The symbols r_+ and r_- indicate that the mode is radiative or nonradiative, respectively.

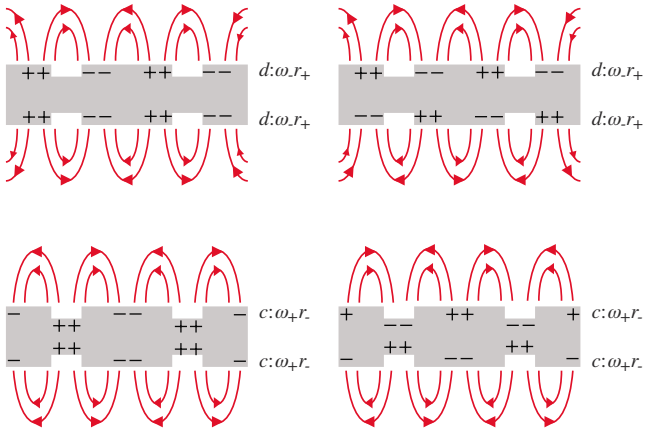

FIG. 5. (Color online) Charge distribution for standing surface plasmons in a corrugated metal film at the band gap energies at $k_x=0$ for the structure shown in Fig. 1(c). The left two figures are for the SRSP modes, while the right two figures are for the LRSP modes.

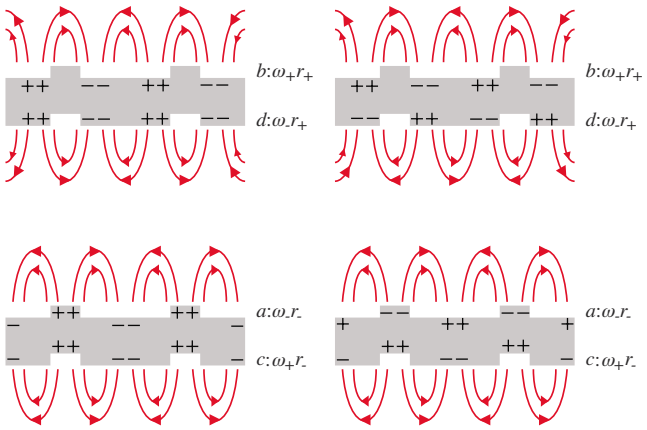

FIG. 6. (Color online) Charge distribution for standing surface plasmons in a corrugated metal film at the band gap energies at $k_x=0$ for the structure shown in Fig. 2(J). The left two figures are for the SRSP modes, while the right two figures are for the LRSP modes.

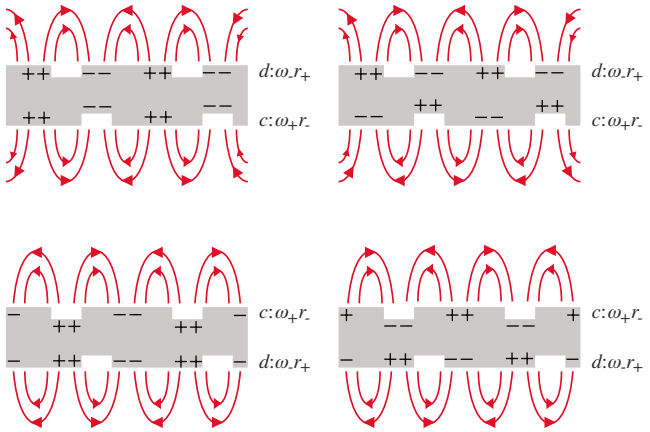

FIG. 7. (Color online) Charge distribution for standing surface plasmons in a corrugated metal film at the band gap energies at $k_x=0$ for the structure shown in Fig. 1(F). The left two figures are for the SRSP modes, while the right two figures are for the LRSP modes.

The electric charge distribution can be deduced from the magnetic field distribution using Maxwell's equations, as shown in Fig. 8(c). Figure 8(d) shows the charge distribution at the upper edge of the same gap. The energy and radiation characteristics of Figs. 8(c) and 8(d) are represented by $[d:\omega_-r_+|a:\omega_-r_-]\rightarrow r_+\omega_{2-}r_-$ and $[c:\omega_+r_-|b:\omega_+r_+]\rightarrow r_-\omega_{2+}r_+$, respectively. Since there is an energy difference, a band gap opens. The modes on both band edges radiate, but this time through different interfaces (compare structures J and L).

The gap behavior in the structures, in which one interface is flat (S, U, V, and X), can also be explained in the same manner. In contrast to all the structures with two corrugated interfaces, each of the three possible band gaps (two intramode band gaps and one intermode band gap) opens at the same time for every structure, but the band gap widths are smaller because of a smaller energy difference between the two charge distributions.

If the film is optically thick and the incident surface is perfectly flat, surface plasmons are never excited by free-space radiation. This is not the case for thin enough metal films if the opposite surface is corrugated—surface plasmons can be excited by light even through the flat interfaces, as shown in Fig. 3. Thus, the plasmon modes also radiate though the flat interfaces due to reciprocity. However, the coupling efficiency between free-space radiation and plasmons through the flat interface is 1 order of magnitude smaller than that through the corrugated interface due to absorption.

IV. DISCUSSION

We have shown above that both the formation of the plasmonic band gaps and the radiation characteristics of the plasmon modes at band edges can be explained in an intuitive manner by considering the charge distributions of the modes. It is time to return to our main problem—based on the results, which of the investigated structures is the best for a plasmonic band gap laser?

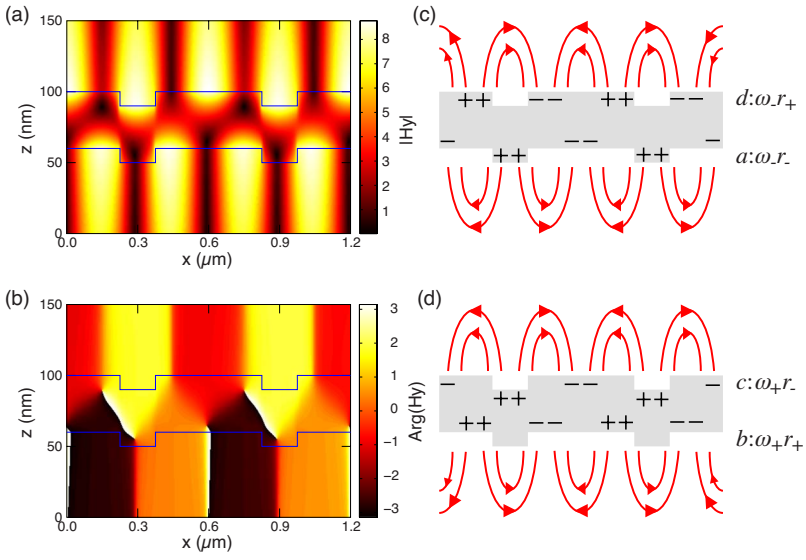

FIG. 8. (Color online) Calculated magnetic field distribution at the lower edge of the intermode plasmonic band gap in the structure shown in Fig. 3(L): (a) amplitude and (b) phase. (c) Corresponding charge distribution to (a) and (b). (d) Charge distribution at the upper edge of the same plasmonic band gap as (c).

As explained before, the basic structure of the laser we proposed is a two-dimensionally corrugated thin silver film coated with a fluorescent laser dye layer on both sides or on one side.[9] In the latter case, the effective dielectric constant of the media on both sides must be identical in order to support LRSP modes.[21] In the proposed laser, the dye pumped by a short pulse laser excites surface plasmon waves with near-field coupling and also produces stimulated amplification of the standing surface plasmon waves at the band edge. A part of the energy of the plasmon is coupled out as a free-space laser beam, which is emitted perpendicular to the surface. In order to realize this laser, the requirements are (1) a wide band gap, (2) a low absorption or internal loss, and (3) a low radiation or scattering loss.

Wide plasmonic band gaps flatten the dispersion curves around the band gap energy, resulting in lowering of the group velocity of the surface plasmons. This brings down the lasing threshold.[10] Therefore, a wide plasmonic band gap is preferable for the plasmonic band gap laser, which is a requirement satisfied by structures A, C, G, H, M, and O.

For the second requirement, i.e., low absorption loss, we have already mentioned the use of the LRSP band gap of a thin film instead of the more lossy plasmon mode on a thick metal surface. All the investigated structures naturally produce LRSP modes—however, the two LRSP band edges differ not only in energy but also in absorption loss. The mode at the upper band edge has smaller absorption losses since it is closer to the light line.[18] Therefore, the upper LRSP band gap edge is the best point for lasing.[20]

Next, we discuss the last requirement, i.e., low radiation loss. In the dispersion maps, as mentioned above, weak absorption indicates weak radiation or low coupling efficiency between surface plasmons and free-space radiation. There is almost no radiation loss at the lower edge of the LRSP (also of the SRSP) band gap in structures A and G, while there is no radiation loss at the higher edge of the LRSP (also of the SRSP) band gap in structures C and I. In these structures, the radiation from both of the interfaces is suppressed at the same edge. On the other hand, there is no radiation loss at the lower LRSP band edge in structure M, while there is no radiation loss at the higher edge of the LRSP band gap in structure O. They are, in fact, the same structure with the incidence interfaces reversed. Thus, in this structure, the radiation loss from both interfaces cannot be suppressed at the same band gap edge.

Based on the above considerations, we conclude that structures C and I are the most appropriate configurations for the plasmonic band gap laser, providing both wide band gap and low losses. However, by taking the actual fabrication process into account, the allure of these structures is somewhat diminished, as the structures with a flat interface are much easier to produce and provide only a slightly smaller band gap. This leads us to conclude that, in practice, structures U and X are the best candidates for achieving a plasmonic laser, and the high-energy edge of the LRSP intramode band gap should be used to minimize absorption losses.

It is worth noting that in addition to LRSP band gaps at normal incidence, intermode band edges may also be used for a plasmonic band gap laser. As pointed out by Winter *et al.*,[22] at the energy of the intramode LRSP band gap edge, the SRSP mode always exists for some nonzero values of wave vector k_x. When exciting LRSPs at this edge by a fluorescent molecule, part of the energy always couples into SRSPs, reducing the gain coefficient of the plasmonic laser. However, at the energy of the intermode plasmonic band gap, there is no other plasmon mode for any value of wave vector k_x so that most energy of the excited dye molecules can be transferred to the desired plasmonic mode. Unfortunately, the absorption loss is notably higher than that of LRSPs, which is a topic that will be expanded in a future paper.

In the actual plasmonic band gap laser, complete plasmonic band gaps, i.e., band gaps in all propagation directions, might be required. Investigation of the behaviors of plasmonic band gaps in two-dimensionally corrugated thin films is underway.

ACKNOWLEDGMENTS

This research was partially supported by the Ministry of Education, Science, Sports and Culture through Grant-in-Aid for Scientific Research (B) (Grant No. 17360033), 2005. J.S. was supported in part by both the Research and Development Project of the Finnish Ministry of Education and the TEKES FinNano Program through Project No. 40321/05.

*okamoto@riken.jp

[1] W. L. Barnes, A. Dereux, and T. W. Ebbesen, Nature (London) **424**, 824 (2003).
[2] E. Ozbay, Science **311**, 189 (2006).
[3] *Near-Field and Surface Plasmon Polaritons*, edited by S. Kawata (Springer, Berlin, 2001).
[4] M. Nezhad, K. Tetz, and Y. Fainman, Opt. Express **12**, 4072 (2004).
[5] J. Seidel, S. Grafström, and L. Eng, Phys. Rev. Lett. **94**, 177401 (2005).
[6] S. A. Maier, Opt. Commun. **258**, 295 (2006).
[7] D. J. Bergman and M. I. Stockman, Phys. Rev. Lett. **90**, 027402 (2003).
[8] M. A. Noginov, G. Zhu, M. Bahoura, J. Adegoke, C. E. Small, B. A. Ritzo, V. P. Drachev, and V. M. Shalaev, Opt. Lett. **31**, 3022 (2006).
[9] T. Okamoto, F. H'Dhili, and S. Kawata, Appl. Phys. Lett. **85**, 3968 (2004).
[10] K. Sakoda, Opt. Express **4**, 167 (1999).
[11] P. Andrew, G. A. Turnbull, I. D. W. Samuel, and W. L. Barnes, Appl. Phys. Lett. **81**, 954 (2002).
[12] I. R. Hooper and J. R. Sambles, Phys. Rev. B **70**, 045421 (2004).
[13] D. Gérard, L. Salomon, F. de Fornel, and A. V. Zayats, Phys. Rev. B **69**, 113405 (2004).

[14] L. Li, J. Opt. Soc. Am. A **13**, 1024 (1996).
[15] L. Li, J. Opt. Soc. Am. A **13**, 1870 (1996).
[16] M. Nevière and E. Popov, *Light Propagation in Periodic Media* (Dekker, New York, 2003).
[17] P. B. Johnson and R. W. Christy, Phys. Rev. B **6**, 4370 (1972).
[18] W. L. Barnes, T. W. Preist, S. C. Kitson, and J. R. Sambles, Phys. Rev. B **54**, 6227 (1996).
[19] D. Gérard, L. Salomon, F. de Fornel, and A. V. Zayats, Opt. Express **12**, 3652 (2004).
[20] T. Okamoto, F. H'Dhili, J. Feng, J. Simonen, and S. Kawata, in *Nanoplasmonics from Fundamentals to Applications*, edited by S. Kawata and H. Masuhara (Elsevier, Amsterdam, 2004).
[21] F. Pigeon, I. F. Salakhutdinov, and A. V. Tishchenko, J. Appl. Phys. **90**, 852 (2001).
[22] G. Winter, S. Wedge, and W. L. Barnes, N. J. Phys. **8**, 125 (2006).